Angle-dependent ultrasonic wave propagation in rocks for estimating high-resolution elastic properties of complex core samples

Daria Olszowska*, *Gabriel* Gallardo-Giozza, *Domenico* Crisafulli, and *Carlos* Torres-Verdín

The University of Texas at Austin, Austin, TX, USA

Abstract. Due to depositional, diagenetic, and structural processes, reservoir rocks are rarely homogeneous, often exhibiting significant short-range variations in elastic properties. Such spatial variability can have measurable effects on macroscopic mechanical properties for drilling and production operations. We describe a new laboratory method for acquisition of ultrasonic angle-dependent measurements of reflected waves that delivers high-resolution, continuous descriptions of P- and S-wave velocity and anisotropy along the surface of the rock sample. Reflection coefficient vs. incidence angle is the main source of information about rock elastic properties. The acquired measurements are matched to numerical simulations to estimate P- and S-wave velocity and density of the porous sample and their variations within the rock specimen, providing continuous descriptions of sample complexity. Data collected from various locations on the rock specimen are subsequently used to construct 2D models of elastic properties along the surface of the rock sample. P- and S-wave velocities estimated with this method agree well with acoustic transmission measurements for most homogeneous rocks. The spatial resolution of the method is limited by receiver size, measurement frequency, and incidence angle. At high incidence angles, the surface area sensitive to the measurements increases and, consequently, the spatial resolution of the corresponding reflection coefficient decreases across neighboring layers.

1 INTRODUCTION

Sedimentary rocks are rarely homogeneous, often exhibiting high degrees of spatial heterogeneity due to various geological processes such as deposition, diagenesis, and tectonics. As exemplified in Figure 1, alternating layers of stiff and compliant rocks, with thicknesses varying from millimeters to meters, pose challenges for drilling and production operations. Knowledge of the mechanical properties of rocks and their spatial variations is crucial for formation strength predictions, wellbore and perforation stability, sand production evaluation, and subsidence problems [1-3]. Presence of heterogeneities below the resolution of standard laboratory/field techniques leads to spatial averaging effects that mask true rock properties. This behavior can lead to significant consequences, such as wellbore failure, or critical differences between hydraulic fracturing models and actual field observations [4-6]. There is a great need to detect changes in rock elastic properties at a fine scale to mitigate exploration and development risks.

Most standard laboratory techniques fail to estimate small-scale variations of rock elastic properties (static and dynamic). Their resolution is often limited by sample size, yielding average values for thinly-laminated rocks. Presence of pre-existing fractures can also exacerbate measurement biases. The latter biases are commonplace in standard rock loading and ultrasonic transmission methods, which can give unreliable results for complex rock samples. A solution to this averaging problem is the introduction of continuous mechanical property measurements along the specimen, which yield more detailed information about sample variability. Such methods already exist but have limited use in the industry.

Fig. 1. Mancos Shale samples. Different colors refer to compliant (dark) and stiff (light) layers.

The scratch test is a method that correlates the force applied to scratch a rock sample with its mechanical properties (unconfined compressive strength and fracture toughness). When compared to standard strength-testing methods, measurements exhibit much higher resolution (1-2 mm) than with conventional procedures. Measured properties, however, can be biased by both sample saturation and friction between the specimen and the cutter. Moreover, the scratch test leaves a small furrow at the tool-sample

* Corresponding author: daria.olszowska@utexas.edu

contact, raising concerns about possible core damage [7]. Another technique that enables high-resolution detection of mechanical property changes along a rock is the indentation test. Elastic properties of a rock sample are estimated using the relationship between load and depth of penetration. The resolution of this method depends on the tip size and ranges from the nano- to macro-scale. Presence of material "pile-up" or "sink-in" around the tip complicates the interpretation of indentation test results. As a consequence, there may be significant differences between true and apparent contact areas, leading to errors in estimated properties [8-10].

We introduce an alternative laboratory method to measure rock elastic properties via a spatially continuous and non-destructive method. Using angle-dependent ultrasonic reflection coefficients, high-resolution data are delivered for rock sample properties and their variability. In the sections that follow, we first describe the new laboratory system and the corresponding measuring technique. Next, angle-dependent ultrasonic reflection coefficients are used to estimate elastic properties along homogeneous and complex rocks (artificial and natural) and to generate 2D descriptions of the examined rock samples.

2 METHOD

The ultrasonic angle-dependent reflection coefficient method is a technique that offers improved resolution compared to standard laboratory measurements. It is a pitch-catch method, where the source and the receivers are positioned at an angle with the sample. Data are collected at multiple incidence angles and the measurements are normalized with a reference value. Continuous measurements performed along the sample mitigate spatial averaging effects. The resolution of our method is determined by both transducer diameter and signal frequency. Because the size of the acoustic beam is much smaller than the sample, the measurement is sensitive to a limited surface area. This area, owing to the nature of the measurement, increases with incidence angle (θ_i) and is proportional to $1/\cos(\theta_i)$. Data are collected at various locations across the sample surface, providing detailed information about rock property changes, and used to construct a 2D rock model.

2.1 Reflection-coefficient measurement system

Figure 2 shows the reflection-coefficient measurement apparatus. The initial design of this apparatus is well described in the literature [11,12]. An update in the design that distinguishes it from other similar devices is the receiver array. Instead of only one receiver and one transmitter, up to four ultrasonic receivers can be used at different locations. Multiple transducers allow the detection of the reflected and refracted P and S waves simultaneously, thereby reducing measurement time. Figure 3 shows the measurement geometry and illustrates a third type of wave that is detected by the system, i.e., the direct wave, which in some cases can interfere with reflected wave measurements. The direct wave, therefore, needs to be considered when calculating reflection coefficients.

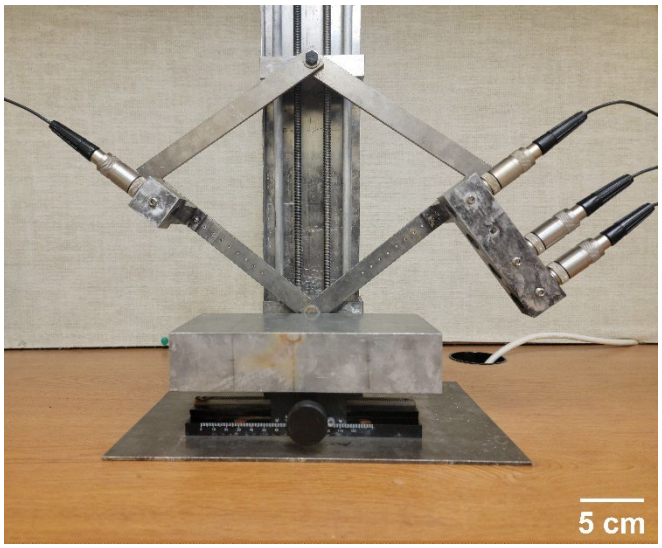

Fig. 2. Ultrasonic reflection coefficient apparatus. The sample (aluminum) is placed on a moving table, allowing changes in sample positioning during the experiment. Transmitter (on the left) and receiver array (on the right) are deployed on two arms with a common rotation axis. Two lead screws allow changes of incidence angle (on the left) and sample top positioning (on the right).

Transmitter and receivers are deployed on two arms with a common axis of rotation attached to two moving plates and lead screws. Such design allows the measurement of reflection coefficients at different incidence angles without moving the sample and while keeping the transducer-sample distance constant. This latter condition ensures that the acoustic beam center be located at the same point for all angle measurements. The rock sample is placed on a moving table allowing measurement-position changes throughout the experiment and continuous data collection along the sample. Two lead screws allow not only variations of incidence angle but also precise sample top positioning.

The laboratory system includes a wave transmission and acquisition module containing an HP 8116A pulse/function generator, Rigol DS1054Z oscilloscope, four Olympus V303 immersion transducers (1 MHz, 1.25 cm diameter), four Olympus V323 immersion transducers (2.25 MHz, 0.64 cm diameter) and watertight transmission cables. Depending on the transducer type, we use 500 ns (1 MHz transducer) or 222 ns (2.25 MHz transducer) pulse signals with 100 Hz repetition frequency and 8 V peak-to-peak amplitude. Each waveform is recorded after performing an average of 256 stacks of measurements in order to mitigate acquisition noise. All measurements are performed with the transducers and the sample submerged in a fluid (water/castor oil).

2.2 Data acquisition, processing, and modeling

The amplitude of the reflected wave and its variation with incidence angle becomes the primary source of rock elastic property information. Reflection coefficients are calculated by comparing the amplitudes of reflected and reference waves. The amplitude of the reference wave is measured by placing the transmitter and receiver face-to-face and

recording the waveform without the presence of the rock sample. This procedure mitigates measurement effects due to transducer size and fluid attenuation. Reflection coefficients are calculated as the ratio of the reflected and reference wave amplitudes. Because the distance traveled by the wave at different incidence angles remains constant, there is no need to correct the measured amplitudes for the effects of attenuation and beam spreading.

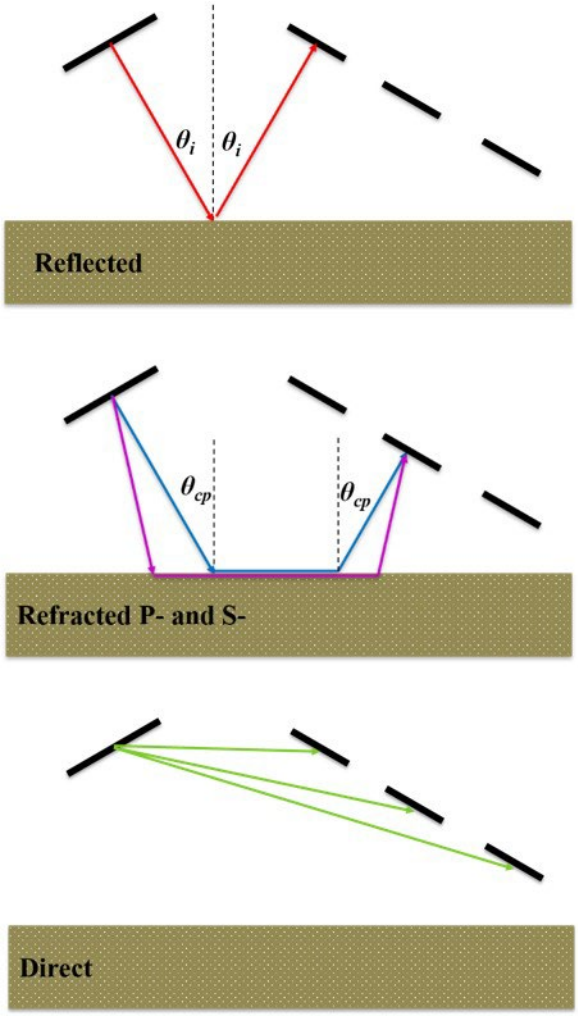

Fig. 3. Wave arrival geometry. A reflected wave propagating at incidence angle θ_i is captured by the first transducer in the receiver array. Measurements are sensitive to a limited surface area. Refracted waves occurring at and beyond P- and S-wave critical angles, θ_{cp} and θ_{cs} (not shown in the figure), respectively, are captured by receivers at positions 2 and 3. Because of the nature of the refracted wave, measurements cover larger surface areas on the rock sample compared to reflection measurements, hence are subject to spatial averaging effects across complex rock samples. Direct waves propagate from the transmitter to the receivers.

Variations of ultrasonic reflection coefficient with angle are then used to estimate rock elastic properties. Measured reflection coefficients are matched with numerical simulations (semi-analytical and numerical models) to estimate P- and S-wave velocities, V_p and V_s, respectively, and density, ρ, of the examined sample. While the semi-analytical model assumes a homogeneous rock sample, the numerical model considers variations in rock elastic properties within the sample. Because of the finite transducer size and source-rock-receiver distance, plane-wave theory cannot be used to describe wave behavior at the interface between two media. Instead, we use a bounded beam model representing the wavefront as a superposition of multiple infinite plane waves traveling in different directions [13]. The acoustic wave is propagated from the source toward the fluid-solid interface using the phase advance technique [14,15], given by

$$P(k_x,k_y,z)= P(k_x,k_y,0)e^{ik_z z} \quad , \qquad (1)$$

where $P(k_x,k_y,0)$ is the source (z = 0) acoustic wavefield, $P(k_x,k_y,z)$ is the acoustic wavefield calculated anywhere in the space, k_x, k_y, and k_z are the wavenumbers in the x, y, and z directions, respectively, and $i = \sqrt{-1}$. At the interface ($z = h$), each plane wave component of the wavefield is modified by the reflection coefficient $R(k_x, k_y)$ in the form

$$P(k_x,k_y,h) = P(k_x,k_y,0)e^{ik_z h}\ R(k_x,k_y). \qquad (2)$$

We use an inhomogeneous wave reflection coefficient model to predict the acoustic wave behavior at the solid-fluid interface [16]. It follows that

$$R(k_x)=\frac{\left(k_s^2-2k_x^2\right)^2+4k_x^2k_{pz}k_{sz}-\frac{\rho_w}{\rho}k_s^4k_{pz}/k_z}{\left(k_s^2-2k_x^2\right)^2+4k_x^2k_{pz}k_{sz}+\frac{\rho_w}{\rho}k_s^4k_{pz}/k_z}, \quad (3)$$

where $k_{pz}=\sqrt{k_p^2-k_x^2}$, $k_p=\frac{\omega}{V_p}$, $k_{sz}=\sqrt{k_s^2-k_x^2}$, and $k_s=\frac{\omega}{V_s}$; k_p and k_s are the P and S wavenumbers in the solid, respectively, ω is the angular frequency, and ρ_w/ρ is the density ratio between the upper and lower media; $R(k_y)$ is calculated using the same equation but changing k_x to k_y. Subsequently, the acoustic wavefield modified by the fluid-solid interface is propagated toward the receiver using the same phase advance technique. Both measurement and modeling schemes, including refracted waves, have been verified with a water-aluminum interface [17]. Results obtained from the latter verification confirmed a good match between measurements and their numerical simulation. Differences between P- and S-wave velocities estimated with the reflection-coefficient method and those measured with a standard acoustic transmission procedure did not exceed 1%. Density, however, was underestimated, with a 7% difference with respect to standard laboratory measurements. The refracted wave method further validated the measurement, yielding an error below 4%.

Complementary to the semi-analytical model, we use SOFI2D (finite-difference viscoelastic time-domain forward modeling algorithm [18,19]) to model reflection coefficients obtained from homogeneous and spatially complex rock samples for their comparison to laboratory measurements. We assume that sample properties change only in one direction. Therefore, in order to reduce computational time, we use a 2.5D model (2D model space with an 3D azimuthal explosive source). The geometry of the laboratory system is replicated by the software. Each reflected wave is normalized

by the reference wave, where the maximum absolute amplitude is the value of the reflection coefficient at a given incidence angle.

3 CASE STUDIES

This section documents the results obtained with the angle-dependent ultrasonic reflection coefficient method using natural and synthetic samples exhibiting homogeneous and heterogeneous elastic properties. Prior to performing the measurements, each sample is first dried in the oven to remove residual fluid saturation and then saturated with water using a vacuum pump. The sample, source, and receiver are submerged in water during the experiment. Based on low-angle reflection coefficient measurements collected at various locations on the sample surface, small-scale variations in reflected wave amplitude are detected and used to construct 2D rock models of reflection coefficient. Likewise, it is shown how angle-dependent reflectivity curves change from one location to another, and how the presence of rock spatial heterogeneity affects the measurements. For the sake of simplicity but without sacrifice of generality, we assume that the sample top is flat and perfectly horizontal and that the distance traveled by the wave remains constant throughout the experiment. Dynamic elastic properties of the tested samples are estimated using a nonlinear inversion algorithm to match measurements with their numerical simulations based on trust-region least-squares minimization [20-22] and compared to standard laboratory measurements when available. The inversion algorithm uses only the absolute value of reflection coefficients to estimate the elastic properties of the rocks. In the following analysis, we assume that rocks are purely elastic/non-dispersive. Phase estimation and modeling requires further analysis of poroelastic rock properties and of their effect on reflected waves. Two types of anisotropic samples are considered for analysis: (1) when layer properties are known before acquiring the measurements (synthetic sample), and (2) when there is no prior information about the sample, layer geometry, and properties.

3.1 Homogeneous samples

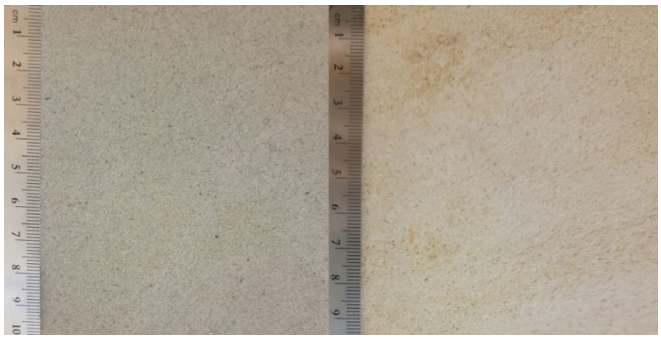

Fig. 4. Homogeneous rock samples. Berea Sandstone (left) and Texas Cream Limestone (right).

This section describes measurements performed on homogeneous rock samples: Berea Sandstone and Texas Cream Limestone. The same rocks are subsequently used to construct synthetic layered samples. Both rock samples are 10x10 cm blocks with a flat surface (Figure 4). Measurements acquired with angle-dependent ultrasonic reflection coefficients are compared against acoustic transmission measurements (Table 1), where source and receiver are placed on opposite ends of the sample and the arrival time of P- and S- waves is measured and translated into V_p and V_s, respectively. For homogeneous samples, we expect the results obtained with both methods to give similar results.

Table 1. Homogeneous samples. Elastic properties measured with the acoustic transmission and ultrasonic reflection coefficient methods and their percentage differences.

Sample	Method	V_p [m/s]	V_s [m/s]	ρ [kg/m^3]
Berea Sandstone	Transmis-sion	2714	1129	2050
	Ultrasonic Reflection Coeffi-cients	2849	1180	1950
	% Differ-ence	5	4.5	5
Texas Cream Lime-stone	Transmis-sion	3355	1775	1920
	Ultrasonic Reflection Coeffi-cients	3402	1649	1845
	% Differ-ence	1.4	7.1	3.9

3.1.1 Berea Sandstone

Figure 5 shows the laboratory results obtained from the water-saturated Berea Sandstone interface. Because of higher data quality and larger signal-to-noise ratio, we choose to only show measurements acquired with 1 MHz transducers. Dashed and dotted lines describe the results obtained with the bounded beam and numerical model, respectively. Table 1 shows the values used to generate both models. The match between measurements and numerical simulation is very good, except at angles from 30 to 35 deg. This discrepancy is related to the P-wave critical angle (31 deg), where the modeled receiver response does not follow the laboratory data trend (increase in measured values); instead, the curve smoothly transitions from an almost horizontal to an inclined orientation. The P-wave becomes inhomogeneous at the longitudinal critical angle, hence part of the energy propagates parallel to the sample surface, while part is converted into a leaky mode, causing disruptions to the wavefield [23]. Differences between properties estimated with the ultrasonic reflection coefficient and the acoustic transmission methods do not exceed 5%.

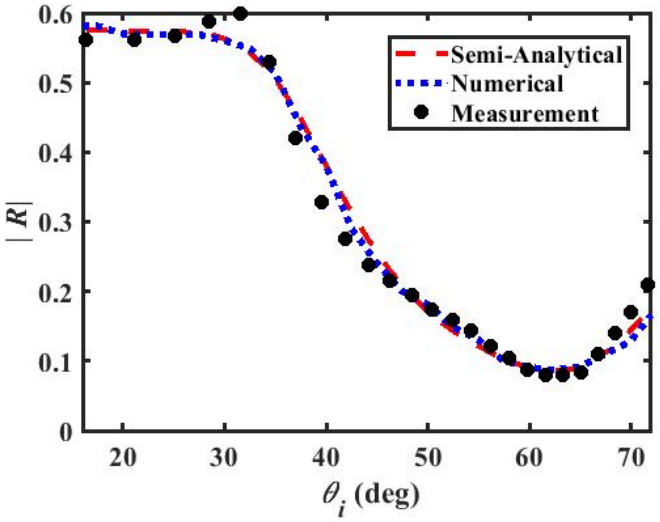

Fig. 5. Berea Sandstone. Measured (dots) and modeled (dashed line – semi-analytical, dotted line - numerical) ultrasonic reflection coefficients with respect to angle of incidence. Measurements performed with a 1-MHz immersion transducers (source and receiver).

3.1.2 Texas Cream Limestone

Figure 6 compares laboratory measurements of ultrasonic reflection coefficients for the Texas Cream Limestone acquired at different incidence angles (dots) against the results obtained with the bounded beam model (dashed lines) and numerical model (dotted lines). Overall, the match between measurements and numerical simulations obtained with both models is good, with some exemptions around 25-30 degrees. Similarly, for the case of Berea Sandstone, results obtained with both numerical models show a discrepancy with laboratory measurements around the P-wave critical angle (23 deg). Numerical simulations show a better fit near the longitudinal critical angle; the amplitude of reflection coefficients increases following the experimental measurements, but their values are lower than those of laboratory measurements. Semi-analytical results exhibit a smooth transition near the P-wave critical angle. Differences between numerical and semi-analytical results are also noticeable at angles above 65 degrees: while the former fit the measurements well, the latter fail to match the experimental data. This behavior coincides with the S-wave critical angle which takes place at 64 degrees. Table 1 describes the elastic properties estimated with the reflection coefficient method, where the results are compared to acoustic transmission measurements. The difference of measurements between the two techniques does not exceed 4%, except for S-wave velocity, which exhibits a difference of 7.1%.

3.2 Complex rock samples

This section describes results obtained for synthetic Berea Sandstone – Texas Cream Limestone and natural complex carbonate samples. A 2D model of the sample is constructed (assuming constant properties within each layer) and the study focuses on how angle-dependent reflectivity curves vary from one data collection location to another and what the effect of the neighboring layers is. In this section, we compare results obtained with two types of transducers, 1 MHz and 2.25 MHz. The difference between the transducers is not only their central frequency of operation but also their size: the 2.25 MHz transducer is half the size of the 1 MHz transducer. We assess the effects of transducer size and frequency on measurement resolution and their ability to estimate properties of a single layer without spatial averaging effects.

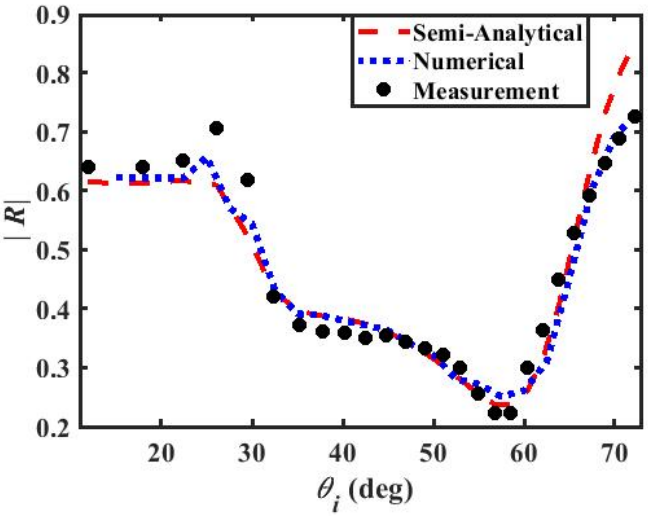

Fig. 6. Texas Cream Limestone. Measured (dots) and modeled (dashed line – semi-analytical, dotted line - numerical) ultrasonic reflection coefficients as a function of angle of incidence. Measurements performed with a 1-MHz immersion transducers (source and receiver).

3.2.1 Berea Sandstone – Texas Cream Limestone

Berea Sandstone – Texas Cream Limestone is an artificial composite stack made of alternating layers of both rocks glued together with epoxy. The thickness of the layers is not constant and varies between 12.5 mm and 21.8 mm. Figures 7A and 7B describe the sample geometry, and the expected reflection coefficients at different locations. For visualization purposes (better color resolution), reflection coefficients are normalized: values range from 0 (for clean Texas Cream Limestone) to 1 (for clean Berea Sandstone). Panels C and D show normalized ultrasonic reflection coefficients obtained at different locations and at very low incidence angles (4 deg) with 1 MHz and 2.25 MHz transducers, respectively. Measurement locations are at the center of each layer and at the boundaries between them as indicated by the black dots. Measurements acquired with both types of receivers indicate variations in the normalized reflection coefficients related to changes in sample property. We observe that numerically simulated reflection coefficients and laboratory measurements do not agree. When the measurement collection point is located at the center of the layer, the reflection coefficient tends to the expected value. On the other hand, at the interface between layers, the measurement is sensitive to both types of rock (averaging effect), whereby the discrepancy with the expected reflection coefficient increases. In general, measurements acquired with higher-frequency transducers show a better match with the Berea

Sandstone/Texas Cream Limestone layered sample model. Differences between the two sets of measurements are caused primarily by transducer size and measurement frequency: the smaller the transducer the higher the resolution.

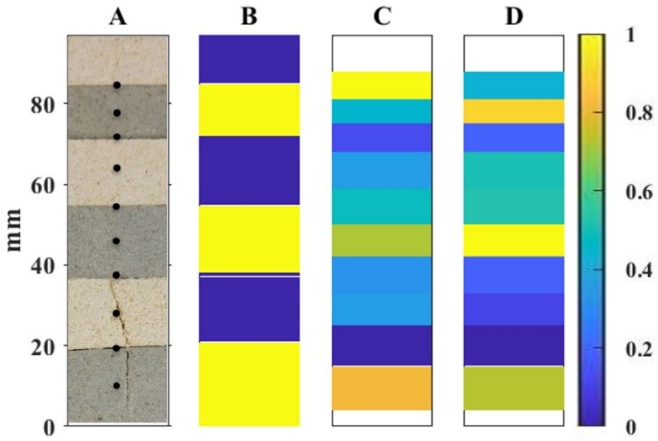

Fig. 7. Artificial complex rock. Panel A shows the sample made of alternating layers of Berea sandstone (grey) and Texas Cream Limestone (light) with measurement locations (dots). Panel B shows expected values of normalized reflection coefficients at different sample locations. Panels C and D show normalized low-angle ultrasonic reflection coefficients measured with 1 MHz and 2.25MHz transducers, respectively.

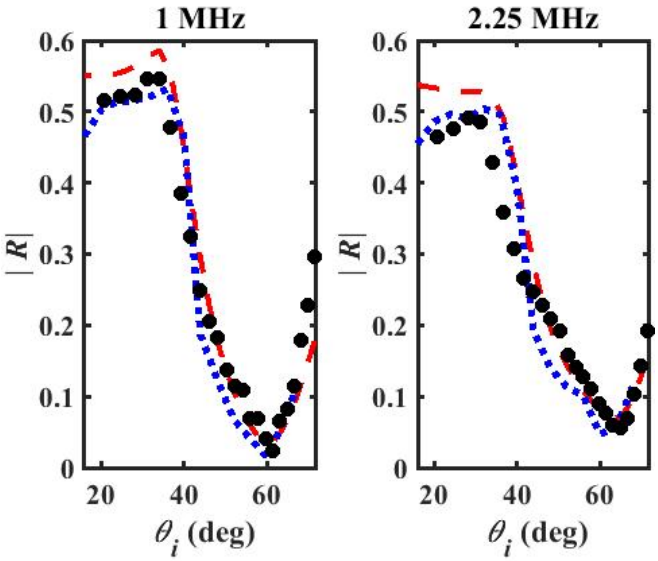

Fig. 8. Center of Berea Sandstone layer (located between 40-55 mm). Measured (dots) and modeled (dashed line – semi-analytical, dotted line - numerical) ultrasonic reflection coefficients as functions of angle of incidence for the cases of 1 MHz (left) and 2.25 MHz transducers (right).

Because angle-dependent reflectivity curves for Berea Sandstone and Texas Cream Limestone have a distinctive shape, we expect to observe differences between the angle-dependent ultrasonic reflection coefficients measured at specific sample locations. Figure 8 compares laboratory measurements acquired with 1 MHz and 2.25 MHz ultrasonic transducers at the center of the 17.3 mm Berea Sandstone layer and their match with semi-analytical numerical simulations. Results obtained with both pairs of transducers have a very similar shape, with small differences between them. Note that the semi-analytical reflection coefficients do not match laboratory measurements performed at low angles for both cases, but the deviation is higher for 2.25 MHz measurements. The numerical model, which contrary to the semi-analytical model includes information about sample heterogeneity, gives a better match at low angles, but deviates from experimental measurements at high angles. Interestingly, we observe that the numerically simulated reflection coefficients change depending on the measurement frequency, even when layer thickness (17.28 mm) is greater than transducer size, confirming the laboratory observations. Elastic properties estimated with both measurements yield similar values when compared to homogeneous Berea Sandstone properties estimated with standard laboratory methods. The difference does not exceed 5%, except for V_S estimated from 2.25 MHz measurements (5.4%). In general, in this case, the 1 MHz measurement yields a smaller difference with respect to homogeneous sample properties.

Figure 9 shows how the measured angle-dependent ultrasonic reflection coefficients change from one measurement location to another. In this example, the center of the beam was placed either in the center of the Berea Sandstone layer (BS2 stands for the second Berea Sandstone sample counted from the bottom) or at the border with Texas Cream Limestone. We describe two cases: when Texas Cream is either on the right (BS2/TX2) or the left side (TX1/BS2) of Berea Sandstone. TX1 and TX2 stand for the first and the second Texas Cream Limestone layer counted from the bottom of the sample, respectively. We observe that reflectivity curves measured with 1 MHz and 2.25 MHz transducers differ, although, they all have a shape that is close to that of the homogeneous Berea Sandstone, without much visible effect due to the Texas Cream Limestone. We expected to observe a greater deviation from the homogeneous sample behavior, especially at the Berea Sandstone/Texas Cream Limestone interface. Measurements acquired with the 1 MHz transducers almost overlap, except between 20 - 40 degrees, where we observe additional discrepancies between the acquired measurements. We know that the area sensitive to the measurement increases with the incidence angle, thereby increasing the sample averaging effect. Therefore, the resolution of the measurement is the highest possible at low angles. We observe more variability in the measurements acquired with 2.25 MHz transducers than with 1 MHz transducers. The increase in amplitude below 40 degrees is much more significant for the measurements acquired at the interface. Additionally, the location of the minimum reflection coefficient is shifted toward higher angles at the center of the layer. When we compare homogeneous Berea Sandstone and Texas Cream Limestone angle-dependent reflectivity curves, we notice that the location of the minimum value changes from 65 degrees to 59 degrees, respectively. The measurement acquired from the center of the Berea Sandstone layer with the 2.25 MHz transducer is sensitive mostly to the properties of the single material, with minimal effect due to neighboring layers. This behavior confirms our previous observations that smaller-diameter and higher-frequency transducers provide enhanced resolution when estimating changes in the sample elastic properties. Although the differences in reflection coefficient plots obtained at different sample locations can be subtle, they

are related to changes in the material density or P/S-wave critical angle. It is also important to note that epoxy used to glue the components has a measurable effect on reflection coefficient measurements. We do not record a smooth transition between the layers; instead, we observe a mechanical discontinuity causing internal reflections and backscattering, thereby increasing the difficulty of interpretation and data–model match.

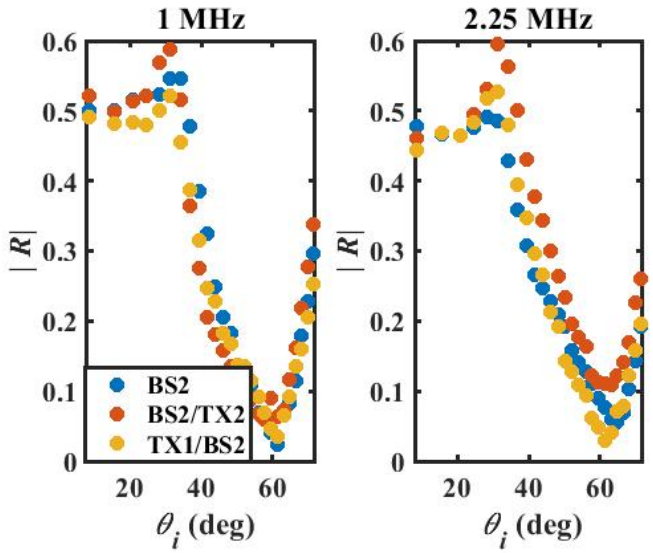

Fig. 9. Angle-dependent ultrasonic reflection coefficients obtained at the center of the Berea Sandstone layer (blue), and at the interface with Texas Cream Limestone (red and yellow). Measurements performed with 1 MHz (left) and 2.25 MHz transducers (right).

3.2.2 Complex carbonate

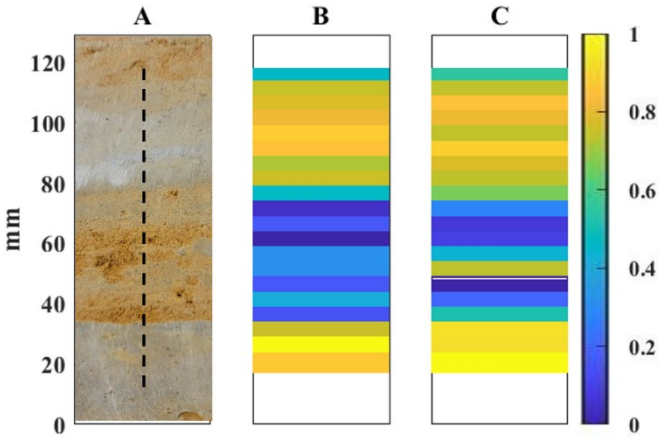

Fig. 10. Complex carbonate. Panel A shows the sample with the measurement axis (dashed line). Measurements are acquired every 5 mm between 10 mm and 110 mm. Panel B shows normalized low-angle ultrasonic reflection coefficients obtained with the 1 MHz transducer. Panel C shows normalized low-angle ultrasonic reflection coefficients obtained with 2.25 MHz transducers.

As shown in Figure 10, the complex carbonate sample is a natural rock with visible layering. Contrary to the artificial sample, there is no prior information about layer elastic properties. From macroscopic observations, we notice that the light gray layers are very tight, with low porosity, while the brown layers have small vugs. Low-angle reflection coefficients measured between 20 mm and 120 mm at 5 mm intervals along the samples show variability across the sample, hence suggesting changes in rock elastic properties. Normalized reflection coefficient plots show regions with high and low values, which correspond to the light grey and brown layers, respectively. This behavior confirms our macroscopic observations: tight areas exhibit higher impedance (higher velocity and density) compared to the vuggy zone. Similar to the previous case, measurements acquired with 2.25 MHz transducers exhibit better resolution; we also observe more variability in the measurements across the sample.

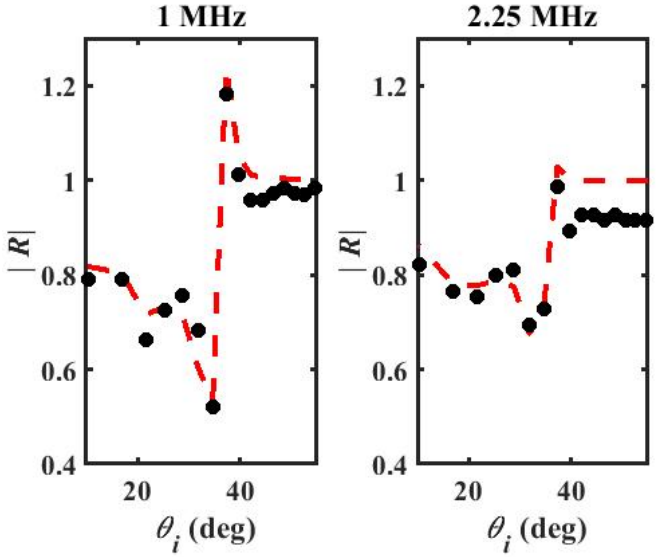

Fig. 11. Complex carbonate. Measured (dots) and modeled (dashed line) ultrasonic reflection coefficients as a function of angle of incidence for 1 MHz (left) and 2.25 MHz transducers (right). The center of the beam is located at 90 mm (approximately the center of the light-gray layer).

Measurements acquired at the center of the light-gray layer (100 mm) with 1 MHz and 2.25 MHz transducers are matched with numerical simulations performed with the semi-analytical model (Figure 11). Angle-dependent ultrasonic reflection coefficients measured with both types of transducers have a similar shape but with a smaller range in the values for the higher-frequency measurements. The bounded beam model has difficulties matching the 2.25 MHz measurements at angles above 40 degrees, and simulated reflection coefficients are higher than the measured reflection coefficients. Despite differences in the experimental angle-dependent reflection coefficients, both measurements yield similar values of P- and S-wave velocities; V_p ranges from 5906 m/s (1 MHz) to 6158 m/s (2.25 MHz), with a 3% difference between the estimated values. S-wave velocity estimated with both measurements gives 2882 m/s and 2893 m/s, for the 1 MHz and 2.25 MHz transducers, respectively (0.3% difference). Density estimations, however, exhibit a

significant difference (28%) between the lower (2434 kg/m^3) and the higher frequency measurements (3114 kg/m^3). Based on a better model-laboratory match obtained for 1 MHz measurements and the expected density of tight carbonate rocks, we conclude that the lower sample density is a more reliable outcome.

Figure 12 shows how angle-dependent reflection coefficients vary across the complex carbonate sample. Measurements are centered at 35, 60, 75, and 100 mm; locations are selected based on both low-angle reflection coefficients (minimum, maximum, and the transition zone) and macroscopic variations in sample properties (visible layers/alteration zones). We observe a significant change in the angle-dependent reflectivity curves between measurement locations related to changes in rock elastic properties. Variations in wave velocities estimated for different sample locations range from 5061 m/s to 6158 m/s for V_p and from 2700 m/s to 2893 m/s for V_s. Those values yield a percentage change of 17.8% and 6.7% in P- and S-wave velocities, respectively.

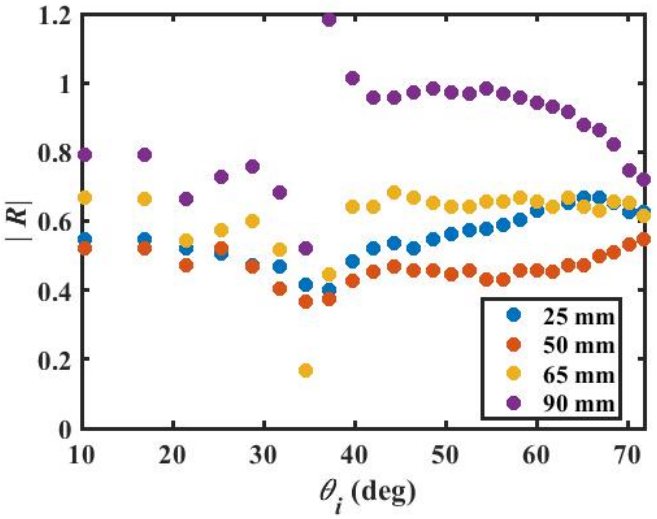

Fig. 12. Angle-dependent ultrasonic reflection coefficients measured at different locations across the complex carbonate sample. Measurements acquired with the 1 MHz transducer.

4 CONCLUSIONS

Ultrasonic angle-dependent reflection coefficient measurements enable high-resolution estimation of rock elastic properties under laboratory conditions. Comparison between measurements, semi-analytical and numerical simulations in homogeneous media show good agreement. Analysis of heterogeneous media shows that the spatial resolution of reflection coefficient measurements increases with increasing frequency and decreasing transducer diameter. This behavior is due to the acoustic beam spread (lower for higher-frequency signals) and the active area of the sensor.

The angle-dependent ultrasonic reflection coefficient method was implemented to estimate elastic properties of four water-saturated samples: (1) homogeneous Berea Sandstone, (2) Texas Cream Limestone, (3) heterogenous synthetic sample made of alternating layers of Berea Sandstone and Texas Cream Limestone, and (4) a complex carbonate with visible layers/alterations. Measurements performed on homogenous rocks were matched with semi-analytical and numerical simulations. Estimated elastic properties compared against standard laboratory methods showed a good agreement, with differences not exceeding 5% for most of the cases. This result confirms the reliability of the ultrasonic angle-dependent reflection coefficient measurements as an alternative method to estimate rock elastic properties.

The method was tested on synthetic and natural complex samples. Low-angle (4 degrees) reflection coefficients measured at different locations across the sample showed variations related to local changes in sample elastic properties. As expected, measurements acquired with smaller transducers exhibited greater spatial variations in the estimated rock properties. Because the measurement is sensitive to a surface area limited by the receiver size, the smaller the transducer the lower the averaging effect in heterogeneous samples. The effect of transducer size on the measurements was also noticeable in the angle-dependent reflection coefficient curves; measurements acquired with a larger diameter receiver exhibited a very similar shape at different locations when the layer thickness was below the sensor resolution. On the other hand, we observed that laboratory measurements acquired with smaller-diameter transducers were in general more difficult to match with semi-analytical or numerical simulations. The drawback of having small transmitter and receivers is the system sensitivity to sample imperfections (e.g. cracks, fractures, not a flat surface) and requires higher precision in sample positioning (the acoustic beam needs to be centered directly at the top of the sample). With this condition, one can estimate the properties of a single layer in a complex sample with an error below 5% when compared to a homogeneous rock of the same type.

5 NOMENCLATURE

h = source – interface distance
i = imaginary unit
k = wavenumber in fluid
k_x = x-component of the wavenumber in fluid
k_y = y-component of the wavenumber in fluid
k_z = z-component of the wavenumber in fluid
k_p = compressional wavenumber in solid
k_{pz} = z- component of the compressional wavenumber in solid
k_s = shear wavenumber in solid
k_{sz} = z-component of the shear wavenumber in solid
P = acoustic wavefield
R = ultrasonic reflection coefficient
V_p = compressional-wave velocity in solid
V_s = shear-wave velocity in solid
x,y,z = coordinates of a cartesian coordinate system
θ_i = incidence angle
θ_{cp} = compressional-wave critical angle
θ_{cs} = shear-wave critical angle
ρ_w = density of the upper medium (water)
ρ = density of the lower medium (sample)
ω = angular frequency

6 ACKNOWLEDGMENTS

This work reported in this paper was funded by the University of Texas at Austin's Research Consortium on Formation Evaluation, jointly sponsored by Aramco, Baker Hughes, BHP Billiton, BP, Chevron, CNOOC International, ConocoPhillips, Eni, Equinor ASA, Halliburton, INPEX Corporation, Occidental, Oil Search, Petrobras, Repsol, Schlumberger, Todd Energy, TotalEnergies, and Wintershall Dea.

7 REFERENCES

1. W.A.M. Wanniarachchi, P.G. Ranjith, M.S.A. Perera, Q. Lyu, B. Mahanta, R. Soc. Open Sci., **4**, 1-10 (2017)
2. E. Fjaer, R.M. Holt, A.M. Holt, P. Horsrud, *Petroleum Related Rock Mechanics* (Elsevier, Oxford, 2008)
3. D.K. Sethi, *SPE/DOE Low Permeability Gas Reservoirs Symposium*, SPE-9833-MS (1981)
4. J.L. Miskimins, R.D. Barree, *SPE Production and Operations Symposium*, SPE-80935-MS (2003)
5. B.V.V Cherian, S. Higgins-Borchardt, G.A.A. Bordakov, A. Yunuskhojayev, Z. Al-Jalal, D. Mata, J. Jeffers, *SPE Energy Resources Conference*, SPE-169960-MS (2014)
6. R. Suarez-Rivera, W.D. Von Gonten, J. Graham, S. Ali, J. Degenhardt, A. Jegadeesan, *Unconventional Resources Technology Conference*, URTEC-2460515-MS (2016)
7. G. Schei, E. Fjaer, E. Detournay, C.J. Kenter, G.F. Fuh, F. Zausa, *SPE Annual Technical Conference and Exhibition*, SPE 63255 (2000)
8. S. Suresh, A.E. Giannakopoulos, J. Alcala, Acta Mater., **45**, 1307-1321 (1997)
9. A.E. Giannakopoulos, S. Suresh, Scr. Mater., **40**, 1191 – 1198 (1999)
10. J. Alcala, A.E. Giannakopoulos, S. Suresh, J. Mater. Res., **13**, 1390 – 1400 (2011)
11. T. Pialucha, P. Cawley, 1994, J. Acoust. Soc. Am., **96**, 1651 – 1660 (1994)
12. J.D Sagers, M.R. Haberman, P.S. Wilson, 2013, J. Acoust. Soc. Am., **134**, EL271 – EL275 (2013)
13. L.M. Brekhovskikh, *Waves in Layered Media* (Nauka, Moscow, 1960)
14. Y. Bouzidi, D.R. Schmitt, 2008, IEEE Trans. Ultrason. Ferroelectr. Freq. Control, **55**, 2661 – 2673 (2008)
15. R. Malehmir, N. Kazemi, D.R. Schmitt, Ultrasonics, **80**, 15-21 (2017)
16. S. Vanaverbeke, F. Windels, O. Leroy, J. Acoust. Soc. Am., **113**, 73 – 83 (2003)
17. D. Olszowska, G. Gallardo-Giozza, C. Torres-Verdin, *SPWLA 62th Annual Logging Symposium*, SPWLA-2021-0058 (2021)
18. T. Bohlen, Comput. and Geosci., *28*, 887–899 (2002)
19. T. Bohlen, D. De Nil, D. Köhn, S. Jetschny, *SOFI2D seismic modeling with finite differences: 2D—elastic and viscoelastic version. Users guide* (Karlsruhe Institute of Technology, Karlsruhe, 2016)
20. K. Levenberg, Q. Appl. Math., **2**, 164–168 (1994)
21. D. Marquardt, SIAM J. Appl. Math., **11**, 431–441 (1963)
22. J.J. Moré, *Conference on Numerical Analysis* (1977)
23. T.P. Pialucha, *The reflection coefficient from interface layers in NDT of adhesive joints* (Imperial College of Science, Technology and Medicine, University of London, 1992)